ENHANCED PERFORMANCE SCALING METHODOLY

Jon E. Eaton, Applied Research Laboratory, Penn State University, USA
Eckard Praefke, Schaffran Propeller & Service GmbH, Germany
Friedrich Mewis, Hamburg Ship Model Basin (HSVA, Germany

FAST 2003, Ischia, Italy
7-10 October, 2003
Papers (Vol. 1), Session A2, page 17-26

ENHANCED PERFORMANCE SCALING METHODOLOGY

Jon E. Eaton, Applied Research Laboratory, Penn State University, USA
Eckhard Praefke, Schaffran Propeller & Service GmbH, Germany
Friedrich Mewis, Hamburg Ship Model Basin (HSVA), Germany

SUMMARY

Due to the increasing popularity of waterjet and multi-component propulsors for high speed marine vessels, applicable performance scaling methodologies are now required for these propulsors. This paper describes a coherent methodology for projecting model to full-scale marine propulsor powering performance applicable to numerous conventional and advanced propulsor configurations. Inclusion of a surface roughness model enables this method to handle a broad range of model and full-scale fabrication classes. Addition of Reynolds number dependent viscous drag models facilitates application to a wide range of propulsor configurations (i.e., open propellers to ducted propulsors). The method is demonstrated by application to recent tow tank test results for a commercial pod and Electric Boat's novel Commercial Rim Drive Pod (RDP) propulsor. Hamburgische Schiffbau-Versuchsanstalt GmbH (HSVA) performed the comprehensive tow tank test program and collaborated with the RDP's hydrodynamic design agent, the Applied Research Laboratory of the Pennsylvania State University (ARL-Penn State), in developing this enhanced performance scaling method.

AUTHOR BIOGRAPHY

Jon E. Eaton is a research engineer and program manager in the Flow & Structural Mechanics Office at the Applied Research Laboratory of Penn State University. His technical expertise is in advanced surface ship and undersea weapon propulsion development and design.

Eckhard Praefke heads the hydrodynamics and propeller design department at Schaffran Propeller & Service GmbH, Lübeck (Germany). His prior experience includes a 15 year career at the Hamburg Ship Model Basin (HSVA) in the areas of propulsor design, manufacturing and testing. He holds a "Diplomingenieur für Schiffbau" from the Technical University of Hannover.

Friedrich Mewis is a Director of the Hamburg Ship Model Basin (HSVA) and head of the Resistance and Propulsion department. Previously, he was employed by the Potsdam Ship Model Basin (SVA). He holds a "Diplomingenieur für Schiffbau" from the University of Rostock, and is a member of the Powering Performance Committee of the 24th ITTC.

1.0 INTRODUCTION

The conventional methodology within the commercial maritime industry is to "scale" model test powering performance data to full-scale values based on the Reynolds number (Re) dependence of skin friction drag, C_D. The pressure (i.e., profile) component of the drag force is assumed to be Reynolds number independent. Typically, the Schoenherr skin friction (alias, ATTC) line, Equation 1, or the ITTC '57 friction line, Equation 2, is employed to approximate the variation in viscous drag losses on ship hulls, Reference 1. In light of these being flat plate drag models (i.e., zero pressure gradient), which ignore the transitional flow regime (i.e., $10^5<Re_c<10^7$), both models yield excessive drag corrections at the low Reynolds numbers of Froude-scale tow tank tests.

$$0.242/\sqrt{C_D} = Log_{10}(\mathrm{Re}_c \cdot C_D) \qquad [1]$$

$$C_D = \frac{0.075}{(Log_{10}\mathrm{Re}_c - 2)^2} \qquad [2]$$

Accordingly, the ITTC '78 propulsor performance scaling methodology, employs a skin friction model of the transitional and turbulent flow regime, Equation 3, that extends to $Re_c = 2x10^5$,

$$C_D = 0.044\,\mathrm{Re}_c^{-1/6} - 5\,\mathrm{Re}_c^{-2/3} \qquad [3]$$

as shown in Figure 1, for application to model scale data. The full-scale drag model assumes the relative surface finish roughness (ε) would exceed the smooth wall approximation and, therefore, uses a "fully rough" drag model, Equation 4.

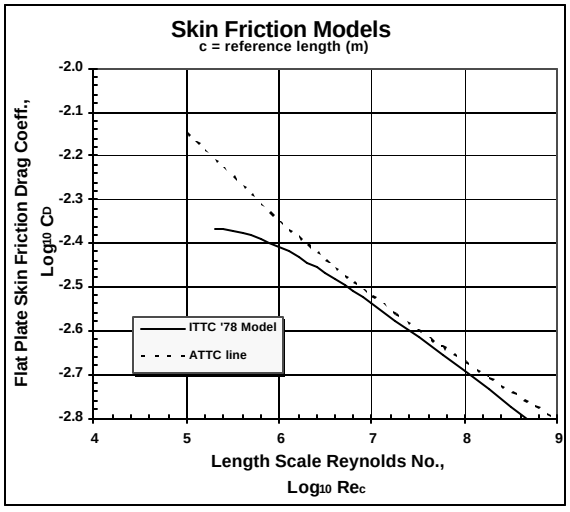

Figure 1: Smooth Wall Skin Friction Models

$$C_{D\,FR} = \left(1.89 - 1.62 Log_{10}\left(e/c\right)\right)^{-2.5} \quad [4]$$

"Fully rough" flow is defined as the condition where the wall surface finish (typically, in units of μm or μ–in.) exceeds the laminar sub-layer height of the turbulent boundary layer. According to the ITTC '78 method, a realistic value of surface finish, including the impact of fouling, is 30μm (1180μ-in.) which is an order of magnitude greater than typical clean wrought/rolled steel plate. The projected difference in model and full-scale skin friction ($C_{D\,MS}$ and $C_{D\,FS}$, respectively) is then related to a difference in section drag coefficient by the following relationship,

$$\Delta C_D = 2\left(1 + 2\left(t/c\right)_{0.75R}\right)\left(C_{D\,MS} - C_{D\,FS}\right) \quad [5]$$

where, *t* and *c* are the propeller section thickness and chordlength at 75% tip radius ($0.75R_P$). This "delta" drag value is then related to variations in the propeller thrust (*T*) and torque (*Q*) coefficients (K_T and K_Q, respectively) by the following empirical expressions,

$$\begin{aligned}\Delta K_T &= K_{T\,FS} - K_{T\,MS} \\ &= \Delta C_D\, 0.3\left(P/D\right)_{0.75R}\left(cZ/D\right)\end{aligned} \quad [6]$$

and

$$\begin{aligned}\Delta K_Q &= K_{Q\,FS} - K_{Q\,MS} \\ &= -\Delta C_D\, 0.25\left(cZ/D\right),\end{aligned} \quad [7]$$

where *P/D* is the pitch-to-diameter ratio at $0.75R_P$ and *Z* is the blade number.

The premise of this scaling methodology, the variation in skin friction drag, is rational, but the employed assumptions/mechanics are problematic for the following issues;

1. The ITTC '78 method assumes that the model hardware will be hydraulically smooth (i.e., polished) and the full-scale trials will be conducted after some propeller fouling has occurred.
2. The Reynolds numbers of typical Froude scale tow tank tests are often limited to $Re \leq 5x10^5$, with the potential risk of laminar separation.

The assumed values of full and model-scale surface finish may not reflect reality for either the model tests or the sea trials. The issue of limited model-scale Reynolds numbers is typically addressed in one of three ways,

1. Assume that the propeller ingests turbulent hull boundary layer flow,
2. Install boundary layer "trips" (i.e., leading edge sand grain roughness or a wire trip) to force or "fix" transition, or
3. Employ a non-polished surface finish to achieve a "fully-rough" wall condition to insure turbulent flow.

The assumption of turbulent inflow is cost effective, but introduces the risk of laminar separation and, therefore, a significant degree of uncertainty in the test results. The application of boundary layer trips is a common practice, but introduces additional drag sources at the risk of contaminating or biasing the measurements. Employing a non-polished, rough-wall finish is a rational compromise, but the finish needs to be measured and documented with the test results. However, a "rough-wall" friction model will be required for the calculation of the model-scale friction drag.

Fundamentally, the ITTC '78 scaling methodology is an empirical method derived from model- and full-scale performance of conventional propellers. As an example, compare Equations 6 & 7 with the following results of a dimensional analysis for the impact of skin friction drag variation on propeller blade torque and thrust,

$$\Delta K_Q \propto -\Delta C_D \left(W/nD\right)^2 EAR\left(r/D\right) \quad [8]$$

and

$$\Delta K_T \propto \Delta C_D \left(W/nD\right)^2 EAR \quad [9]$$

where

W is the relative flow velocity,
n is the rotation rate (rps) and
EAR is the expanded area ratio of the propeller,
EAR = $(Z/p)\int(c/R)d(r/R)$.

Equations 8 & 9 are applicable to any blade row, avoiding the inherent preferences/prejudices of an empirical relationship. Similarly, the ITTC '78 method treats the shaft, bearing barrels and support struts as elements of the hull and scaled as the hull resistance, ignoring the impact of the propeller's induced flow field on theses appendages. Accordingly, this approach is inadequate for waterjets, ducted units and, possibly, podded propulsors where the propulsor induced flow field will dominate the flow patterns over the propulsor appendages.

As described in Reference 2, Eckhard Praefke of Schaffran Propeller proposed a more unified scaling method consisting of spanwise integrated propeller drag loads based on a common friction line model. Later, Friedrich Mewis of HSVA, who employed this technique during a systematic evaluation of podded propulsors, suggested using this technique on the additional wetted surfaces of advanced propulsor configurations. In the case of podded propulsors, such as the AziPod™ and Mermaid™, this method applies to the propeller and pod body, yielding a correction for the unit or net thrust. This method offers a more coherent approach than the ITTC '78 method and is adaptable to any friction line model (i.e., ATTC, ITTC '78, etc.). Traditionally, HSVA has used the ATTC line, which provides a reasonable approximation of their in-house fabricated propeller models (surface finish (ε) ~3μm or 125μ-in.) which are, typically, scaled to full-scale Reynolds numbers of $Re = 10^7$.

The premise of an enhanced scaling methodology would be an extension of Praefke's approach with a small, but comprehensive, collection of drag models such that the calculation methodology would be common to all propulsor types. In this manner, the methodology will be

a consistent procedure, applicable to a broad range of propulsor configurations and avoiding empirical biases.

2.0 RECENT EFFORT: ENHANCED PERFORMANCE SCALING METHOD

Predicated on the Praefke's approach, this paper presents a coherently formulated skin friction drag scaling procedure, the "Enhanced Performance Scaling (EPS) Method", which includes Reynolds number and surface finish roughness effects. The intended benefits of the EPS method are;

1. Broad configuration applicability
   High grade commercial marine propulsors are typically fixed or controllable pitch propellers of moderate blade area ($0.5 < EAR < 0.7$), that operate at modest advance ratios, $0.6 < J_A < 1.0$. Unfortunately, these assumptions are not applicable to many fast ship propulsors, such as water-jets or high advance ratio, $J_A > 1.4$ (i.e., high shaft torque), multi-component propulsor configurations. In both cases, there are multiple propulsor components and it is difficult to conduct Froude-scale tow tank tests at adequate Reynolds numbers to insure turbulent flow on all wetted surfaces of the propulsor. Although $Re \sim 500{,}000$ is the desired minimum test condition, practical limitations may dictate tow tank testing at lower Reynolds numbers, in the transitional flow regime. This is an issue for all wetted surfaces of the propulsor (i.e., blade rows, ducts, etc.), but especially the stationary components. Accordingly, the EPS method includes skin friction drag models for the laminar, transitional and turbulent flow regimes.

2. Compensation of model finish variation
   Many tow tank and, especially, water tunnel test facilities, such as ARL-PENN STATE, use or fabricate polished propulsor models to avoid erratic model-scale cavitation performance. However, it is also common for model propellers to be produced without a polished surface finish to limit model fabrication costs. Therefore, it is quite probable that performance comparisons will be based on tow tank test results from units with significantly different surface finishes. Accordingly, the philosophy applied to the model to full-scale performance scaling needs to be applied to the variation in model scale surface finish.

3. Adaptability to full scale surface finish
   Analogous the model scale testing, the full-scale surface finish will impact sea trial results. Accordingly, the scaling methodology must be adaptable to the propulsor surface finish at the time of the at-sea trial.

The first step in this effort was the development of a smooth wall skin friction model extending from the laminar to turbulent flow regimes. The laminar flow solution performed by H. Blasius (1908) provides the drag model for low Reynold's number flows, $Re_c \le 10^5$,

$$C_{DLam} = 1.328 \mathrm{Re}_c^{-0.5} \qquad [10]$$

In the turbulent flow regime, $Re_c \ge 10^7$, Prandtl's drag model is employed,

$$C_{DTurb} = 0.455 (Log_{10}\ \mathrm{Re}_c)^{-2.58}, \qquad [11]$$

which is a common approximation of the ATTC line at $Re_c = 10^7$. The transitional flow model was developed as a smooth transition from the ITTC '78 model-scale drag model at low Reynolds numbers to the ATTC line at Reynolds numbers approaching $Re_c \to 10^7$. For completeness, the new transition friction drag model,

$$Log_{10} C_{D\ Trans} = -0.05364 (Log_{10} \mathrm{Re}_c)^2 + 0.5710 (Log_{10} \mathrm{Re}_c) - 3.891, \qquad [12]$$

extends to the laminar flow line at $Re_C = 10^5$, and minimizes any "theoretical" local minima (i.e., "drag bucket") at the intersection of the laminar and transitional drag characteristics.

The resulting EPS smooth wall drag model is shown in Figure 2. The final element in the drag model

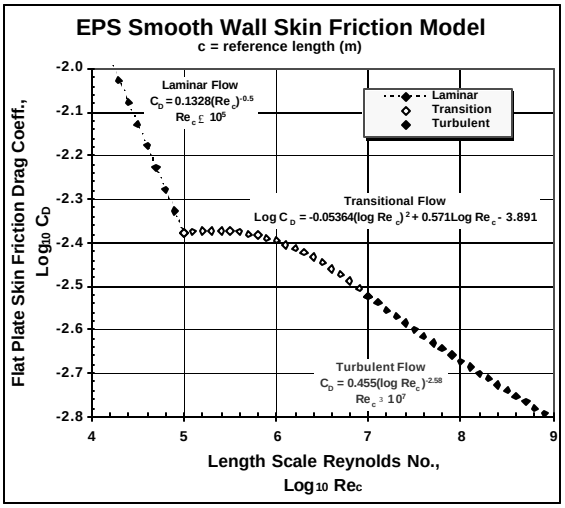

Figure 2: EPS Smooth Wall Skin Friction Model

development was the inclusion of a surface finish drag model. The rough wall drag model attributed to Prandtl and Schlichting (1934), Reference 3, is used,

$$C_{DFR} = (1.89 - 1.62 Log_{10}(e/c))^{-2.5}, \qquad [13]$$

where e is the surface finish and c is the reference length scale. This is the same relationship employed in the ITTC '78 full-scale drag model. The surface finish employed in Equation 13 is a sand grain roughness which is assumed equivalent to the amplitude or 141% of the root-mean-square (rms) measure of the surface finish. The combination of the smooth and rough wall friction models is shown graphically in Figure 3. For simplicity, the transition region between smooth and "fully rough" wall flow conditions has been ignored.

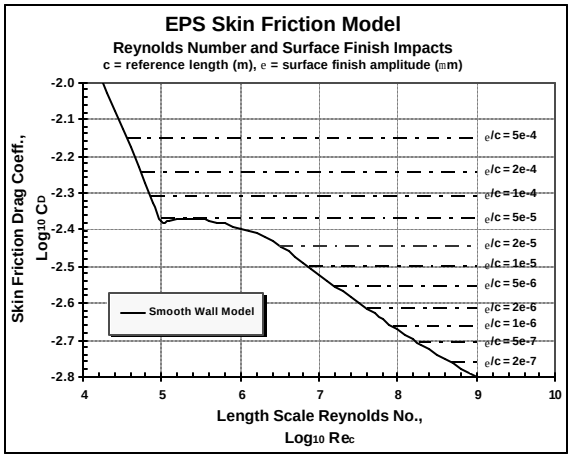

Figure 3: EPS Skin Friction Model

2.1 BLADE ROW APPLICATION

An attractive feature of Praefke's method is the spanwise integration of propeller viscous drag. A step-wise integration correlates the drag model, the blade row geometry (i.e., blade number and spanwise distribution of chordlength) and the local flow field.

$$C_{D\,BladeRow} \propto Z\int C_{Di}\left(\frac{W_i}{V_A}\right)^2\left(\frac{c_i}{R_P}\right)d\left(\frac{r}{R_P}\right), \quad [14]$$

$$\propto Z\sum\left[\overline{C_{Di}}\left(\overline{\frac{W_i}{V_A}}\right)^2\left(\overline{\frac{c_i}{R_P}}\right)\Delta\left(\frac{r}{R_P}\right)\right]$$

where the subscript i indicates local values.

The local relative velocity, chordlength and surface roughness are used to calculate the local skin friction drag coefficient, C_{Di}. Ideally, the propulsor design agent provides the geometry details and the predicted design point velocity distributions for these calculations. The EPS method retains this feature with a few modifications to expedite the calculation of the off-design values of efficiency variation, $\Delta\eta = \eta_{FS} - \eta_{MS}$, such that the extent of model scale performance data (i.e., bollards to zero net thrust) can be scaled. The initial step in the EPS method is the design point integration of the model and full-scale drag induced thrust (C_{DT}) and torque (C_{DQ}) loads shown in the following equations.

$$C_{DT} = \frac{T_{DragFriction}}{\frac{r}{2}V_A^2 p R_P^2}$$

$$\approx \frac{-4\cdot Z}{p}\sum\left[\overline{C_{Di}}\,Cos\left(\overline{b}\right)\left(\overline{\frac{W_i}{V_A}}\,Cos\left(\overline{b}-\overline{a}\right)\right)^2\overline{\frac{c_i}{R_P}}\;\overline{\frac{\Delta r_i}{R_P}}\right] \quad [15]$$

$$C_{DQ} = \frac{Q_{DragFriction}}{rV_A^2 p R_P^3}$$

$$\approx \frac{2\cdot Z}{p}\sum\left[\overline{C_{Di}}\,Sin\left(\overline{b}\right)\left(\overline{\frac{W_i}{V_A}}\,Cos\left(\overline{b}-\overline{a}\right)\right)^2\overline{\frac{c_i}{R_P}}\;\overline{\frac{r_i}{R_P}}\,\frac{\Delta r_i}{R_P}\right] \quad [16]$$

where

T = Blade row thrust/drag
Q = Blade row torque
b = local section stagger angle
= 90°-section pitch angle, $\angle_P$
a = local relative flow angle referenced to the axial direction.

The quantity $Cos(b\text{-}a)$ references the friction drag load to the blade chord line. Although it is feasible to use Equations 15 and 16 for the calculation of the off-design drag loads, the EPS method uses a $0.7R_P$ approximation to simplify the calculations. Based on the design point integrated values, the variations in full and model-scale thrust and torque coefficient are calculated

$$\Delta C_{DT} = C_{DT\,FS} - C_{DT\,MS} \quad [17]$$

$$\Delta C_{DQ} = C_{DQ\,FS} - C_{DQ\,MS} \quad [18]$$

and correlated to approximate values based on the blade row geometry and flow velocities at $0.7R_P$. The expressions for the approximate relationships are given in Equations 19 & 20.

$$\Delta C_{DT\,Approx} = -4\left[\left[\overline{C_D}\,Cos\left(\overline{b}\right)\left(\overline{\frac{W}{V_A}}\,Cos\left(\overline{b}-\overline{a}\right)\right)^2 EAR\right]_{FS} - \left[\overline{C_D}\,Cos\left(\overline{b}\right)\left(\overline{\frac{W}{V_A}}\,Cos\left(\overline{b}-\overline{a}\right)\right)^2 EAR\right]_{MS}\right]_{0.7R_P} \quad [19]$$

$$\Delta C_{DQ\,Approx} = 2\left[\left[\overline{C_D}\,Sin\left(\overline{b}\right)\left(\overline{\frac{W}{V_A}}\,Cos\left(\overline{b}-\overline{a}\right)\right)^2 EAR\frac{r}{R_P}\right]_{FS} - \left[\overline{C_D}\,Sin\left(\overline{b}\right)\left(\overline{\frac{W}{V_A}}\,Cos\left(\overline{b}-\overline{a}\right)\right)^2 EAR\frac{r}{R_P}\right]_{MS}\right]_{0.7R_P} \quad [20]$$

The correlation factors, $k_{\Delta T}$ and $k_{\Delta Q}$ are calculated as,

$$k_{\Delta T} = \Delta C_{DT} \Big/ \Delta C_{DT\,Approx} \quad [21]$$

and

$$k_{\Delta Q} = \Delta C_{DQ} \Big/ \Delta C_{DQ\,Approx}, \quad [22]$$

based on the design point values. Thus, the following expressions for drag induced thrust and torque change can be stated;

$$\Delta C_{DT} = -4k_{\Delta T} \times \left[\left[\overline{C_D}\, Cos\left(\overline{b}\right) \left(\frac{\overline{W}}{V_A} Cos\left(\overline{b} - \overline{a}\right) \right)^2 EAR \right]_{FS} - \left[\overline{C_D}\, Cos\left(\overline{b}\right) \left(\frac{\overline{W}}{V_A} Cos\left(\overline{b} - \overline{a}\right) \right)^2 EAR \right]_{MS} \right]_{0.7R_P} \quad [23]$$

and

$$\Delta C_{DQ} = 2k_{\Delta Q} \times \left[\left[\overline{C_D}\, Sin\left(\overline{b}\right) \left(\frac{\overline{W}}{V_A} Cos\left(\overline{b} - \overline{a}\right) \right)^2 EAR \frac{r}{R_P} \right]_{FS} - \left[\overline{C_D}\, Sin\left(\overline{b}\right) \left(\frac{\overline{W}}{V_A} Cos\left(\overline{b} - \overline{a}\right) \right)^2 EAR \frac{r}{R_P} \right]_{MS} \right]_{0.7R_P} \quad [24]$$

Since the model and full scale blade rows are homologous, Equations 23 and 24 can be restated as;

$$\Delta C_{DT} = -4k_{\Delta T} \left[Cos\left(\overline{b}\right) \left(\frac{\overline{W}}{V_A} Cos\left(\overline{b} - \overline{a}\right) \right)^2 \times EAR\left(\overline{C_{D\,FS}} - \overline{C_{D\,MS}}\right) \right]_{0.7R_P} \quad [25]$$

and

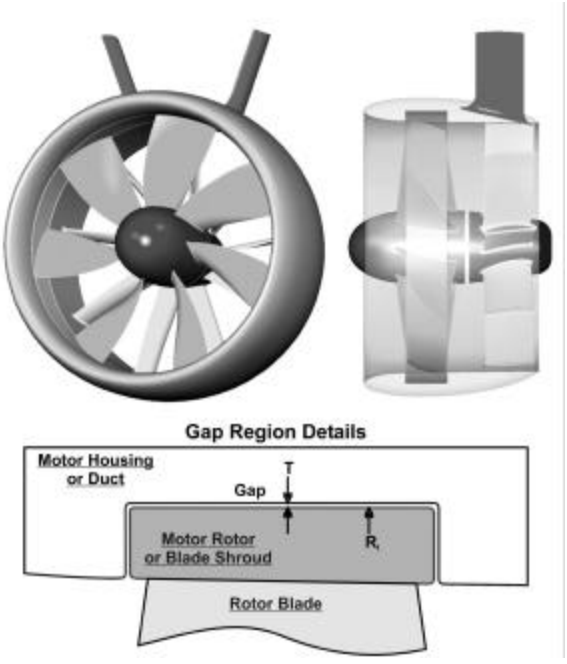

Figure 4: Rim Drive Pod Propulsor, Gap Region Details, Reference 6

$$\Delta C_{DQ} = 2k_{\Delta Q} \left[Sin\left(\overline{b}\right) \left(\frac{\overline{W}}{V_A} Cos\left(\overline{b} - \overline{a}\right) \right)^2 \times EAR\left(0.7\right)\left(\overline{C_{D\,FS}} - \overline{C_{D\,MS}}\right) \right]_{0.7R_P} \quad [26]$$

when a common model and full-scale advance ratio is maintained. With the addition of a mutually agreeable off-design velocity model, $W/V_A = f(J_A, K_T, \text{etc.})$, Equations 25 and 26 provide a means of calculating the change in skin friction induced loads for the range of model-scale data.

2.2 ANCILLARY WETTED SURFACES

Beyond the blade rows, the thrust and torque corrections for the propulsor's remaining wetted surfaces are calculated in a similar manner. The thrust correction is the axial component of the skin friction drag variation, Equation 27, while the torque correction is based on the tangential component, Equation 28.

$$\Delta C_{DT} = -\left(\overline{C_{D\,FS}} - \overline{C_{D\,MS}}\right) \left(\overline{Cos\left(\overline{a}\right)} \frac{W}{V_A} \right)^2 \frac{A_{Wet}}{A_{Prop}} \quad [27]$$

$$\Delta C_{DQ} = 2\left(\overline{C_{D\,FS}} - \overline{C_{D\,MS}}\right) \left(\overline{Sin\left(\overline{a}\right)} \frac{W}{V_A} \right)^2 \frac{A_{Wet}}{A_{Prop}} \frac{r_{Eff}}{R_P} \quad [28]$$

where $A_{Prop} = \pi R_P^2$

Since the variation in torque load on the propulsor's stationary components does not impact the calculation of propulsor efficiency, the calculation of these quantities is typically ignored in the scaling calculations.

2.2.1 ROTOR GAP REGION SURFACES

The rotor gap region flow fields of advanced propulsor configurations, such as waterjets, with rotor tip shrouds or rim-driven propulsors/thrusters, as shown in Figure 4, present additional complications to the calculation of the model and full-scale drag losses. While the drag load on the inboard surface of the shroud/rim can be calculated with the flat plate drag model, the outboard surface and end faces (axial gap regions) of the shroud/rim rotate in the restricted gap region where the clearance (T) is, probably, less than an equivalent flat plate boundary layer height, $\delta_{BL} \sim (0.14 \sim 0.16) c (Re_c)^{-1/7}$. Accordingly, the drag loads on the rotating surfaces of the gap region require specialized models to maintain validity of the procedure. Viable drag models have been identified for the outboard and end-face surfaces, but do not include surface finish correlations. These models are described in the following.

2.2.1.1 CYLINDRICAL OUTBOARD SURFACE

The rotor/shroud outboard surface drag calculation was derived from the Taylor-Couette flow models of Bilgen and Boulos, Reference 4. Based on their experiments and historical data, Bilgen and Boulos developed a cylinder moment characteristic, shown in Figure 5,

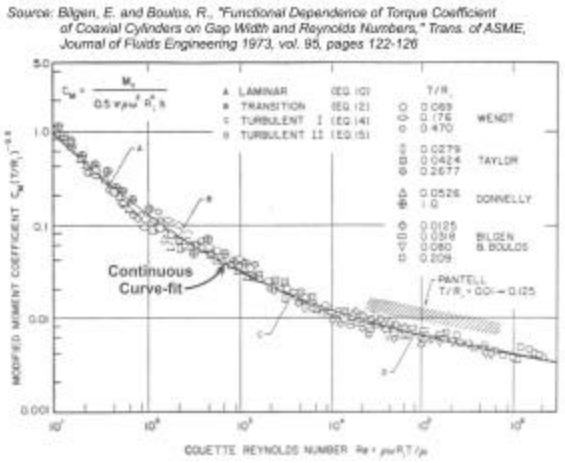

Figure 5: Outboard Cylinder Moment Characteristics: Taylor-Couette Flow

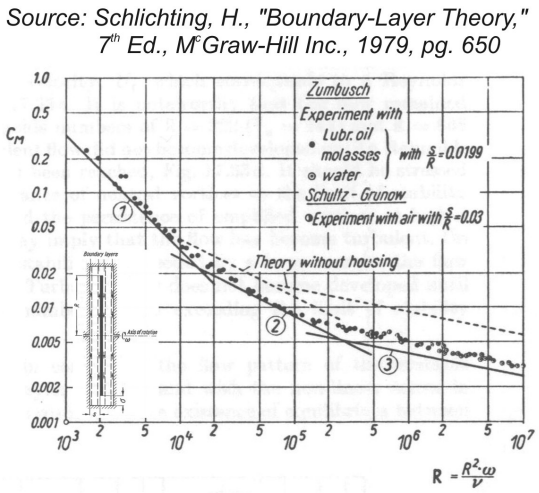

Figure 6: Enclosed Rotating Disk Drag

relating the moment coefficient, C_M, and relative gap clearance (T/R_i) to a Couette Reynolds number, $Re_T=\omega R_i T/\nu$. The authors modeled the compiled results as four (4) linear segments. As shown in Figure 5, the EPS method substitutes a continuous 3rd order curve-fit for the segmented model. Following the convention of the EPS method, the curve-fit model, Equation 29, is stated in terms of a skin friction drag coefficient, where $C_{DQ} = 0.5C_M$ (the Q subscript indicates that this drag will be a torsional load).

$$Log_{10}\left(\frac{C_{DQ}}{\left(T/R_i\right)^{0.3}}\right)=\begin{pmatrix}-0.009419\left(Log_{10}\mathrm{Re}_T\right)^3\\+0.1819\left(Log_{10}\mathrm{Re}_T\right)^2\\-1.343\left(Log_{10}\mathrm{Re}_T\right)\\+0.8526\end{pmatrix} \qquad [29]$$

Admittedly, this model ignores the impact of the pressure driven mass flow through the gap and cannot address the effect of surface roughness. However, based on computational analysis (axisymmetric Reynolds Averaged Navier-Stokes (RANS) code), the velocity of the gap region mass flow is limited to less than 1% of the propulsor inlet velocity, V_A. Therefore, the model is assumed to be an adequate approximation.

2.2.1.2 END FACES

The end face drag model is derived from Schlichting's model for a spinning disk of radius R_i in an enclosure/casing, Reference 5. A graphical comparison of the reference analytic and experimental data is shown in Figure 6. In the range of practical application to model-scale propulsors, where Reynolds numbers exceed $Re_{Ri} = \omega R_i^2/\nu > 1\sim2x10^4$, the rotating disk drag is independent of the axial clearance gap. In the range, $\sim1x10^4 < Re_{Ri} < \sim2x10^5$, the flow is laminar and the analytical solution for moment coefficient (both faces of the disk), $C_{MDisk} = 2.67Re_{Ri}^{-0.5}$ (where $C_{MDisk} = 2Q/[(\rho/2)(\omega R_i)^2 R_i^3]$), agrees well with experimental data. In the turbulent flow regime, $Re_{Ri} > \sim2x10^5$, the presented analytic model, $C_{MDisk} = 0.0622Re_{Ri}^{-0.2}$, is noted to under-estimate the measured disk moment by ~17%. Employing this observation and noting that the characteristic slope of the model and experimental data are similar, allows one to propose $C_{MDisk} \sim (0.0622/0.83)Re_{Ri}^{-0.2} \sim 0.075Re_{Ri}^{-0.2}$ as an empirical model.

Therefore, in terms of the EPS method, the moment coefficient, C_{MDisk}, is related to a torsional drag coefficient, C_{DQ}, for a single face by the following expression.

$$C_{DQ}=\frac{Q}{\frac{r}{2}\left(wR_{Eff}\right)^2 2pR_{Eff}^2\Delta R} \qquad [30]$$

$$=\frac{\left(\frac{C_{M\ Disk}}{2}\right)\frac{r}{2}w^2\left(R_i^5-R_{ii}^5\right)}{\frac{r}{2}\left(wR_{Eff}\right)^2 2pR_{Eff}^2\Delta R}$$

where

R_i = Rotor shroud outer radius
R_{ii} = Rotor shroud inner radius
DR = Shroud span, R_i- R_{ii}, and
R_{Eff} = Effective radius, R_i-DR/2.

Based on the definition of R_{Eff}, Equation 30 can be restated as,

$$C_{DQ}=\frac{C_{M\ Disk}}{4p}\left(\frac{R_i^5-R_{ii}^5}{\Delta R\left(Ri-0.5\Delta R\right)^4}\right), \qquad [31]$$

which in the laminar flow case, $Re_{Ri} < \sim2x10^5$, yields

$$C_{DQ}=0.213\mathrm{Re}_{Ri}^{-0.5}\left(\frac{R_i^5-R_{ii}^5}{\Delta R\left(Ri-0.5\Delta R\right)^4}\right) \qquad [32]$$

or, in the turbulent case, $Re_{Ri} > \sim2x10^5$,

$$C_{DQ}=0.00596\mathrm{Re}_{Ri}^{-0.2}\left(\frac{R_i^5-R_{ii}^5}{\Delta R\left(Ri-0.5\Delta R\right)^4}\right). \qquad [33]$$

As in the case of the case of the rotor shroud outboard surface, this drag model is limited to a smooth wall approximation.

3.0 APPLICATION OF EPS METHOD

The EPS method was applied to recent tow tank open water test results for a "state-of-the-art" conventional pod, (i.e., AziPod™, Mermaid™ or Dolphin™ configuration) and the advanced rim-drive pod (RDP), shown in Figure 4 and described in Reference 6. Electric Boat funded the development, design, model scale testing of the RDP. For brevity, the conventional pod configuration is identified as a hub driven pod (HDP) in this paper. The tow tank data was collected during a comparative evaluation of these two concepts for a panmax cruise vessel. The 1/25th scale test program was conducted by HSVA at their facilities in Hamburg, Germany. Both units are 18~20MW designs capable of 24+ knot maximum speeds. HSVA projects full-scale cavitation-free speeds of 20~21knots for both units. The HDP unit has a 5.8m screw with an expanded area of EAR = 0.65~0.70. The RDP duct has a similar maximum diameter, 5.85m, but the rotor tip diameter (i.e., the inner diameter of the motor rotor) is 4.9m. The blade area of the 7-blade RDP rotor is EAR = 0.785. Due to the increase in stationary and rotating wetted surface area, the RDP is a low RPM (i.e., high advance ratio, J_A ~ 1.60) unit to limit the associated parasitic torque loads.

Following the tow tank test program, an initial sizing effort was performed using an adaptation of Praefke's method for both the RDP and HDP units. Those initial calculations used the ITTC '78 method for the rotor blade rows and applied the ATTC friction model to the remaining stationary and rotating wetted surfaces of the propulsors. The results of that effort were reported in Reference 6. In light of the disjointed nature of the initial scaling effort, ARL-PENN STATE worked in conjunction with Eckhard Praefke and HSVA to develop this "enhanced" scaling method, which will, hopefully, reduce the ambiguity in projecting full-scale propulsor performance.

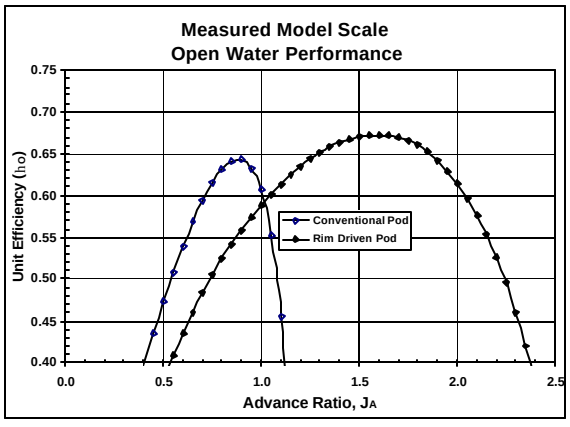

Figure 7: Open Water Test Results

A comparison of the measured HDP and RDP model-scale open water unit efficiencies is shown in Figure 7. The unit efficiency is based on HSVA's net pod thrust (T_{Net}) convention, where

$$T_{Net} = T_{Rotor} - Drag_{Pod\ \&\ Strut}. \quad [34]$$

and

$$h_O = (T_{Net} V_A)/(Qw). \quad [35]$$

Based on these model-scale results, the unit efficiency of the RDP is 2.9 points higher than the HDP (i.e., 67.2% vs. 64.3%). In relative terms, the model-scale RDP is 4.5% more efficient than the HDP. Thus, the primary impetus for the EPS scaling methodology development is obvious. If the RDP and HDP were of similar configuration, the RDP's model-scale performance gain would have been projected to a similar full-scale gain. Unfortunately, the existing scaling models, based solely on parasitic propeller torque loads, are inadequate for a low RPM, multi-component propulsor. A secondary, but important factor is the ambiguity about model scale surface finish. The open water testing of the HSVA fabricated RDP was conducted with an estimated 3.2 μm (125 μin.) surface finish. The HDP open water performance was measured during a previous test program, but there was no measurement, or indication of surface finish. During the subsequent behind hull tests; the HDP unit was delivered to HSVA from another research laboratory with polished propeller blades. As a result, the surface finish variation introduced some ambiguity to the comparison of the HDP and RDP model-scale performance.

The EPS scaling methodology results will be presented in three parts. The first segment will compare the scaled open water efficiency, $\eta_{O\,FS}$ & $\eta_{O\,MS}$ at an estimated design advance ratio ($J_{A\,HDP}$ ~ 0.90 and $J_{A\,RDP}$ ~ 1.6), and indicate the relative sources of the efficiency change. This effort will assume a rough finish model (ε_{MS} = 3.2μm) and a clean/smooth full-scale unit (ε_{FS} = 3.2μm) for both units. The second segment assesses the impact of surface finish by comparing of the projected full-scale design point open water efficiency of the following cases;

1. Polished model (ε_{MS} = 0.5μm), clean full-scale unit (ε_{FS} = 3.2μm),
2. Polished model (ε_{MS} = 0.5μm), fouled full-scale unit (ε_{FS} = 30μm),
3. Rough finish model (ε_{MS} = 3.2μm), clean full-scale unit (ε_{FS} = 3.2μm), and
4. Rough finish model (ε_{MS} = 3.2μm), fouled full-scale unit (ε_{FS} = 30μm).

The final segment will be a comparison of the projected full-scale open water efficiency for the extent of the model-scale advance ratio range. This is referred to as the "off-design" open water efficiency, $\eta_O = f(J_A)$. As in the first segment, this effort will assume a rough finish model (ε_{MS} = 3.2μm) and a clean/smooth full-scale unit (ε_{FS} = 3.2μm) for both units.

3.1 SCALED DESIGN POINT EFFICIENCY

Due to the hydrodynamic and geometry differences, the HDP and RDP units achieved stable characteristics (i.e., Reynolds number independent) at differing values of rotor speed. The HDP open water tests were conducted at 12.02rps while the RDP tests were performed at 16.01rps. At the estimated design advance ratios, the HDP rotor blade Reynolds number was $5.3x10^5$ based on the $70\%R_P$ geometry and relative velocity. The corresponding model-scale Reynolds number for the RDP unit was $4.1 x10^5$.

These model scale values were scaled to a 21-knot full-scale condition assuming that they maintained a constant advance ratio, J_A. The results are listed in Table 1 and indicate a similar, 2.9~3, percentage point change for both configurations. In addition, the projected full-scale efficiency of the HDP unit is consistent with industry experience. Figure 8 shows the relative contribution of each propulsor element to the efficiency scaling. The relatively low advance ratio of the HDP propeller and large pod body area result in large frictional losses for those components and yield significant efficiency changes with Reynolds number. In relative terms, the HDP strut is a minor factor in the efficiency scaling. The results for the RDP unit are fundamentally similar. The RDP motor rim, especially the inboard surface (which experiences the highest relative flow velocities in the unit), is the source of a 1.35 percentage point efficiency gain. The wetted surface area of the duct yields an additional ~0.9 point gain. The scaling of the RDP stator, hub and strut drag indicate minor changes in model to full-scale efficiency due to those components.

Table 1: Scaled Design Point Efficiency - Constant Advance Ratio

Unit	HDP	RDP
Advance Ratio, J_A	0.9	1.6
Model-Scale		
Prop Reynolds Number, $Re_{0.7R}$	$5.3x10^5$	$4.1x10^5$
Open Water Efficiency, η_O	64.3%	67.2%
Full-Scale		
Prop Reynolds Number, $Re_{0.7R}$	$4.6 x10^7$	$1.8 x10^7$
Open Water Efficiency, η_O	67.2%	70.2%
Efficiency Increase, $\Delta\eta_O$	2.9%	3.0%

Notes;

1) Surface finish: Model, $\varepsilon_{MS} = 3.2\mu m$ (rough)
Full-scale, $\varepsilon_{FS} = 3.2\mu m$ (clean)

2) Reynolds number referenced to rotor blade chord and relative velocity at $70\%R_P$

3) $V_A = V_S(1-w)$ where $w = 0.075$

In a separate effort, a computational analysis of the RDP gap region flow field was performed to determine the volume of bypass flow and drag losses at model and full-scale Reynolds numbers. This effort was performed with an axisymmetric RANS code and predicted a 1.88 percentage point efficiency gain due to the rim viscous drag load variation between model and full-scale. The boundary of this computational effort split the rim into; 1) an inner surface consisting of the inboard face and 2) an outer surface consisting of the end faces and the outboard surface. The computational analysis assumed a smooth-wall condition on all surfaces. The computational result exceeded the EPS method projection on both the inner and outer surfaces. In the case of the computational outer surface (end faces and outboard surface), the EPS method predicted a $\Delta\eta = 0.72$ point efficiency gain versus 0.93 for the RANS analysis. On the inner surface, the EPS method prediction was $\Delta\eta = 0.65$ points versus 0.95 for the computational method. In both cases, the computational predictions exceed those of the EPS method by 0.2~0.3 points. Considering the differences in cost and effort to calculate the values, the conservative estimate offered by the EPS method appears to be a viable/cost effective option.

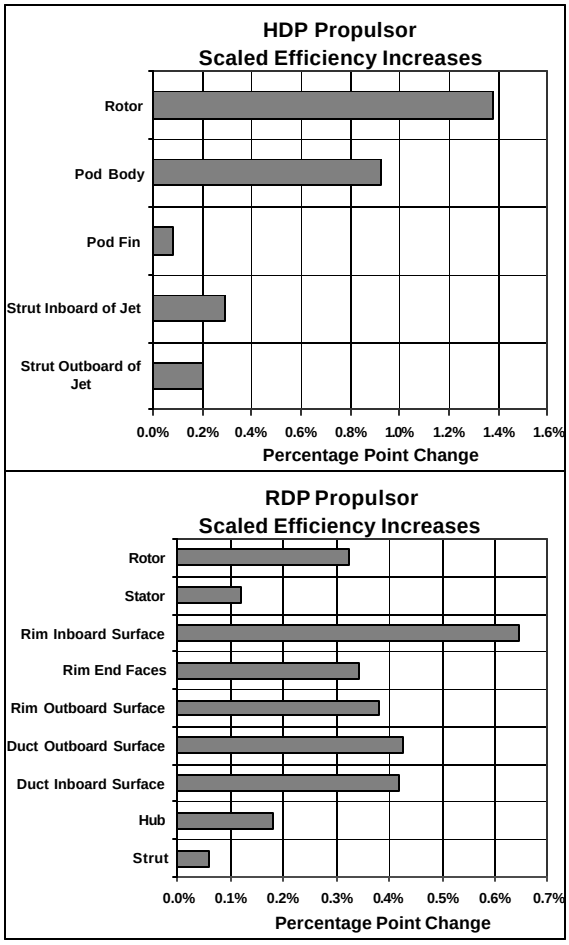

Figure 8: Component Sources of Scaled Efficiency

The combined impact of model and full-scale surface finish is shown in Figure 9. In the case of the EPS

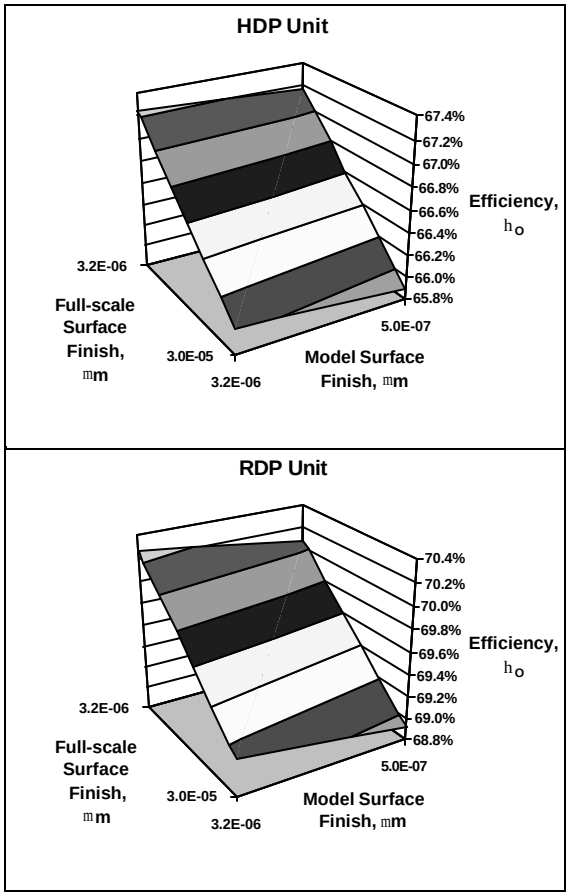

Figure 9: Projected Full-scale Open Water Efficiency

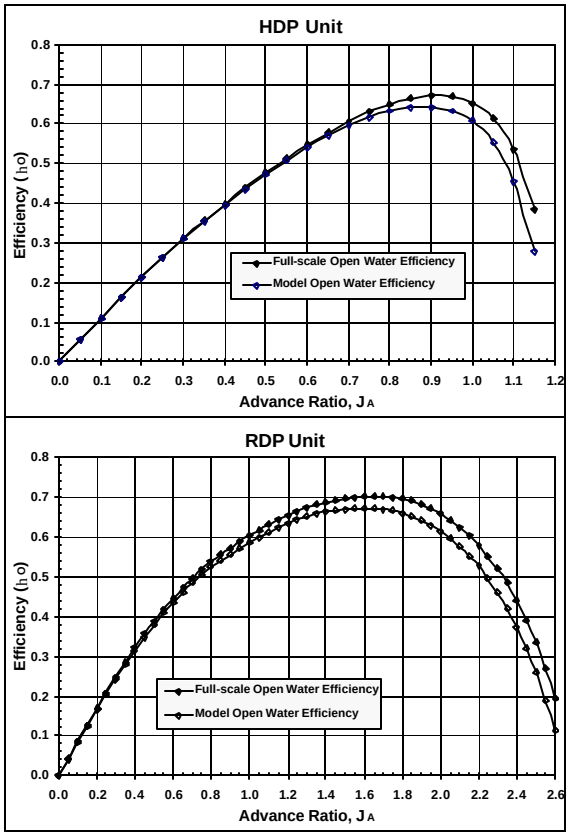

Figure 10: Projected Full-scale Open Water Efficiency

method, the impact of model surface finish is minor relative to that of the full-scale hardware. The EPS smooth wall drag model is conservative (i.e., large skin friction drag coefficients) at model-scale Reynolds numbers and provides a low threshold for a "hydraulically" smooth condition. As an example, the HDP propeller satisfied the smooth wall criteria with a 3.2μm surface finish. The RDP model rotor exceeded the smooth wall criteria (ε_{MS} = 2.2μm would have corresponded to a smooth-wall condition) with a projected efficiency impact of ~0.2 percentage points. Relative to full-scale surface finish, the results shown in Figure 9 are as expected. A rough surface finish on the full-scale hardware will minimize the projected efficiency gains.

3.2 SCALED OFF-DESIGN EFFICIENCY

The off-design calculation uses a "mutually agreed to" model to estimate the propulsor through-flow velocities at off-design advance ratios. In the case of the HDP unit, the propulsor jet velocity, V_J, was based on the actuator disk model, $V_J = V_A(1+C_T)^{0.5}$, where C_T is the thrust coefficient, $C_T = \text{Thrust}/((\rho/2)V_A^2\pi R_P^2)$. In the case of the RDP, which is a constant flow rate machine, the internal and discharge velocities are linear functions of the rotor rotational speed. The duct external surfaces and struts experience the local reference or near-field velocity, V_A. Based on these models, the model and full-scale component drag loads are calculated as a function of advance ratio, yielding a full-scale performance prediction for the range of model-scale open water data. The projections for the rough model, clean full-scale case are shown in Figure 10. Larger efficiency gains are predicted on the right hand side of the maximum efficiency point due to the relative magnitude of the frictional drag verses the propulsor thrust and torque loads as the advance ratio range extends towards the zero thrust condition.

4.0 CONCLUSIONS

1. The presented performance scaling methodology provides a coherent means of estimating the potential efficiency gains/losses associated with variations in Reynolds number and surface finish between model- and full-scale propulsors. The adaptability of the method is demonstrated by its application to recent tow tank open water test results for a "state of the art" commercial pod and an advanced rim driven pod. The projected efficiency gains for the commercial pod are consistent with industry experience. Comparison with computational results indicates that the projected values will be conservative, but reasonable.

2. The viability of this method is dependent on the conservative smooth-wall drag model. Highly polished model propulsors (surface finishes $\varepsilon < 1\mu m$) may delay transition to higher Reynolds numbers than predicted by this model. In which case, the predicted reduction in skin friction drag coefficient will be excessive and, therefore, overestimate the increase in efficiency between model and full-scale. Accordingly, a standard convention for model surface finish is recommended for the industry.

3. Currently, the EPS method does not address the impact of discrete roughness elements (i.e., boundary layer trips and added sand roughness) or isolated surface defects. The scaling methodology pertains to the effects of Reynolds number and surface finish variation between model and full-scale propulsors. However, in the event that viable Reynolds number correlations are developed or identified for discrete disturbances and isolated roughness elements, those relationships would be useful additions to the EPS method.

5.0 REFERENCES:

1. LEWIS, E. V., *Principles of Naval Architecture*, 2nd ed., The Society of Naval Architects and Marine Engineers, 1988

2. PRAEFKE, ECKHARD, "Multi-component Propulsors for Merchant Ships - Design Considerations and Model Test Results; Appendix A: Scale Effect", SNAME symposium "Propellers/Shafting '94", Viginia Beach, VA, USA, September 1994.

3. WHITE, F. W., *Viscous Fluid Flow*, McGraw-Hill, Inc. 1974

4. BILGEN, E AND BOULOS, R. "Functional Dependence of Torque Coefficient of Coaxial Cylinders on Gap Width and Reynolds Numbers, " *Trans. Of ASME, Journal of Fluids Engineering 1973*, vol 95, pages 122-126

5. SCHLICHTING, H., *Boundary-Layer Theory*, 6th and 7th editions, McGraw-Hill, Inc.,1968 & 1979

6. LEA , M., THOMPSON, D., VAN BLARCOM, W., EATON, J., RICHARDS, J., "Scale Model Testing of a Commercial Rim-Driven Propulsor Pod", SNAME Annual Meeting, September 2002